[PROC. OF JSCE No. 344/ I -1 (Structural Eng. /Earthquake Eng. ) April 1984]

# A PRELIMINARY STUDY ON POLYHEDRAL MEMBRANE-PANEL DOMES

*By Hiromichi HIGASHIHARA* and Hiroshi KIKUCHI***

Polyhedral elastic membrane panels are studied with a finite element method. These panels are supposed to be elements of polygonal domes. Membranes generally suffer large deformation and wrinkling; their behaviour is highly nonlinear and introduction of numerical methods is indispensable.

The effect of the wrinkling is well formulated by means of the combination of the incremental loading method and the load transfer method. These two methods define a hierarchical iteration procedure. The method is validated by applying to simplest problems whose solutions have been established by the conventional analyses.

A hexagonal membrane panel is examined in detail which is one of the most fundamental elements of the polygons. Finally, the method presented is applied to a model dodecahedral dome and its mechanical properties are discussed.

## 1. INTRODUCTION

Recent development of material properties of fiber-reinforced plastics (FRP) is suggesting their promising future as structural materials. They are suited above all to light weight structures. As an element of light weight structures FRP is most appropriately applied as membranes.

Theory of membranes has long been discussed and basic equations have been established as early as 1960's[1]. Mechanical behaviors of membrane strtctures, however, do not yet have been fully made clear. Difficulty lies mainly not in the formulation but in the solution procedures.

One major obstacle is geometrical nonlinearity caused by large deflection; basic equations obtained are extremely nonlinear and even simplest problems require numerical treatment. In this paper pentagonal or hexagonal curved membranes are investigated. Problems associated with such simple boundary conditions yet require large computational efforts.

Another obstacle originates from the unique characteristics of membranes, wrinkling. The classical membrane theory mentioned above has carefully kept away from the problem of wrinkling. Only a few simplest problems have been solved analytically[2)~6)]. Some of them are referred later in Chapter 4 in order to examine the numerical method developed in the present study. Wrinkling problem has been so far discussed in the name of tension field[7),8)].

A concept of membrane dome is presented in this paper. It is a polyhedral dome whose faces are pentagonal or hexagonal panels. The idea is described in the next chapter. In Chapter 3 a finite element approach is proposed and its iteration procedures are defined. In Chapter 4 some simplest wrinkling problems which have been solved analytically are treated numerically by the proposed method and its applicability is examined. Analysis of a hexagonal membrane panel is presented in Chapter 5. The proposed method is finally applied to a dodecahedral dome

* Member of JSCE, Dr. Eng., Asst. Prof., Univ. of Saitama (Urawashi, Shimo-ohkubo 225, Saitama)
** Member of JSCE, M. Eng., Shimizu Construction Company, Ltd. (Chuoku, Kyobashi 2-16-1, Tokyo)

in Chapter 6. Because of computational limitation we cannot but be content at present with this miniature. Basic properties of the model as well as the efficiency of the method are discussed.

## 2. CONCEPT OF STRUCTURE

Space structures made of FRP have first been developed as spherical radar domes. Before FRP has been put into practice, they had been constructed as metal space trusses. FRP as radar domes has the virtue of little disturbing the passing electro-magnetic waves. FRP domes have first been introduced as spherical shell. In order to afford bending stiffness, paper honeycomb was sandwiched between curved FRP plates.

Since FRP is most readily fabricated as flat membrane, it is quite natural to compose the dome of flat membranes ; the dome is therefore a polyhedron. Lacking inherent stiffness, it must be supported by internal pressure. This idea has once already been put into practical use[9]. Each panel, a pentagon or a hexagon, consists of a web membrane and surrounding flanges. It can be fabricated at once as one body. The panels are assembled to a dome on the spot simply by connecting pairs of flanges with bolts (Fig. 1). The present study tries to offer a theoretical basis to this concept of structure.

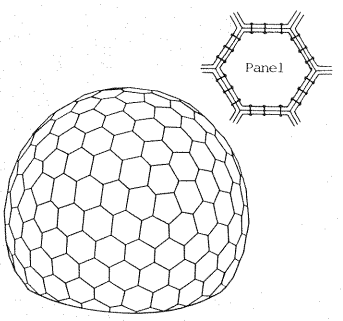


Fig. 1 Concept of Structure.

## 3. FINITE ELEMENT FORMULATION

A lot of problems must be investigated before applying our concept to large structures : plasticity, anisotropy, viscoelasticity (creep problem), and fatigue. All these are to be settled eventually. At first, however, the overall stiffness of the structure is to be made clear. In subsequent discussions the membrane is assumed linearly elastic and isotropic. In this paper, therefore, nonlinear behaviors due to large deflection and wrinkling are the major points in question.

Finite element formulation is employed. Above mentioned nonlinear properties of material are expected to be most systematically taken into consideration by this method. Once an appropriate program is available to the above defined problem, it is easily extended only by changing the stiffness matrix. Since the original program cannot but introduce an iterative procedure, this modification brings about no more difficulties. Finite element method has been recently applied to wrinkling problem of elastic flat membranes[10),11)]. Linear shape functions are exclusively employed in this study. Availability of these simplest functions distinguishes the membrane surface from the shell surface.

### (1) Flat Membrane

If the deformation is small, planar strains are given as

$$\{\varepsilon_0\}=\left(\frac{\partial u_1}{\partial x},\ \frac{\partial u_2}{\partial y},\ \frac{\partial u_1}{\partial y}+\frac{\partial u_2}{\partial x}\right)^T \quad \cdots\cdots(1)$$

The principal strains $\varepsilon_1$ and $\varepsilon_2$ ($\varepsilon_1 \geqq \varepsilon_2$) are equal to

$$\frac{1}{2}(\varepsilon_{01}+\varepsilon_{02})\pm\frac{1}{2}\sqrt{\{(\varepsilon_{01}-\varepsilon_{02})^2+\varepsilon_{03}^2\}} \quad \cdots\cdots(2)$$

If $\sigma_2$ is not negative, this expression holds to the membrane ; i. e., the membrane remains regularly elastic and there is no wrinkling. Principle of the virtual work holds as

$$\int\int\int \sigma_0\delta\varepsilon_0 dV=\int\int \delta u_i f_i dS. \quad \cdots\cdots(3)$$

Introducing the relations $\{\varepsilon_0\}=[B]\{u\}$ and $\{\sigma_0\}=[D]\{\varepsilon_0\}$,

$$\int\int\int [B]^T[D][B]\{u\}\,dV=\{f\}. \quad \cdots\cdots(4)$$

If $\sigma_2$ is negative, the relation (4) no more holds. Since the smaller principal stress vanishes in this case,

$$\varepsilon_2=-\nu\varepsilon_1. \quad \cdots\cdots(5)$$

The unique stress component, the larger principal stress $\sigma_1$, is equal to $E\varepsilon_1$. The principle of the virtual work (3)

is modified as

$$\iiint \sigma_1 \delta\varepsilon_1 dV = \iint \delta u_i f_i dS. \quad (6)$$

Introducing the relation $\delta\varepsilon_1 = \{\Theta\}^T [B] \delta\{u\}$,

$$\iiint [B]^T \{\Theta\} \sigma_1 dV = \{f\}, \quad (7)$$

where $\{\Theta\} = (\cos^2\theta,\ \sin^2\theta,\ \sin\theta\cos\theta)^T$ and $\theta$ is the angle of the direction of the principal stress from the x-axis.

(2) Inflated Membrane

If a normal pressure is applied to the membrane, it moves out of the initial plane. By introducing second order terms of the normal displacement $w$,

$$\{\varepsilon\} = \{\varepsilon_0\} + \{\varepsilon_*\}, \text{ where } \{\varepsilon_*\} = \left\{\frac{1}{2}\left(\frac{\partial w}{\partial x}\right)^2,\ \frac{1}{2}\left(\frac{\partial w}{\partial x}\right)^2,\ \frac{\partial w}{\partial x}\frac{\partial w}{\partial y}\right\}^T. \quad (8)$$

Increment of the strain is expressed in terms of the displacement as

$$\Delta\{\varepsilon\} = ([B] + [A][G])\,\Delta\{u\}_e \quad (9)$$

$$\text{where } [A] = \begin{bmatrix} \frac{\partial w}{\partial x} & 0 & \frac{\partial w}{\partial y} \\ 0 & \frac{\partial w}{\partial y} & \frac{\partial w}{\partial x} \end{bmatrix}^T \text{ and } \begin{Bmatrix} \frac{\partial w}{\partial x} \\ \frac{\partial w}{\partial y} \end{Bmatrix} = [G]\{u\}_e, \quad (10)$$

where the suffix e indicates the element under consideration.

Substituting this relation into the principle of the virtual work (4) and (7),

$$\iiint ([B] + [A][G])^T \{\sigma\}\, dV = \{f\}, \text{ if there is no wrinkling,} \quad (11)$$

$$\text{and } \iiint ([B] + [A][G])^T \{\Theta\}\, \sigma_1 dV = \{f\}, \text{ if there is wrinkling.} \quad (12)$$

Tangent stiffness matrix derived from these relations is given in Appendix II.

Second order terms of the planar strains can be introduced without difficulty. If the inflated membrane suffers very large deflection, these terms play a significant role. Effect of the second order terms of the planar strains stays, however, out of discussion in this paper, because only relatively moderate loads which are expected from the actual natural loads are applied.

(3) Iteration Procedures

By discretizing the basic relations derived in the preceding sections, we eventually obtain a system of non-linear algebraic equations of the form

$$\{k\}(\{u\}) = \{f\}. \quad (13)$$

It is to be noted that the operator $\{k\}$ defines the tensile component of the equivalent nodal force which would be caused by the displacement $\{u\}$ if the field were perfectly elastic.

If the vector-valued function $\{k\}$ has derivatives at $\{u\} = \{u\}_0$,

$$\{k\}(\{u\}_0) + [K]_0(\{u\} - \{u\}_0) = \{f\} \quad (14)$$

for an appropriate domain of $\{u\}$, where $[K]_0 = \left[\frac{\partial k}{\partial u}\right]_0$ is the Jacobian matrix. This expression immediately defines an iteration process:

$$\{u\}_{j+1} = \{u\}_j + [K]_j^{-1}(\{f\} - \{k\}(\{u\}_j)). \quad (15)$$

This is the Newton-Raphson method. Alternatively it may be called a variable stiffness method.

The modified Newton-Raphson method is also available:

$$\{u\}_{j+1} = \{u\}_j + [K]_*^{-1}(\{f\} - \{k\}(\{u\}_j)), \quad (16)$$

where the matrix $[K]_*$ is the tangent stiffness matrix at a tentatively fixed point.

There is a third alternative way. The operator $\{k\}$ can be interpreted, as mentioned above, as the tensile component of the internal force caused by the displacement $\{u\}$. In a similar way can be defined another operator $\{k\}$ which describes the complementary component, the compression, of the internal force. These two nonlinear operators sum up to the stiffness matrix $[K]$ of the corresponding perfectly elastic body; the basic equation takes the form

$$[K]\{u\}=\{f\}+\{k_-\}(\{u\}). \quad \cdots\cdots (17)$$

If the operator $[K]^{-1}\{k_-\}$ is a contraction mapping, this equation is fixed-point type ; it defines a convergent iteration process :

$$\{u\}_{j+1}=[K]^{-1}\{f\}+[K]^{-1}\{k_-\}(\{u\}_j). \quad \cdots\cdots (18)$$

Applying the ordinary incremental iteration procedure to this equation, the so-called no-tension algorithm is obtained which has been applied to no tension materials[12]. Although our problem is a "no-compression" analysis, quite a similar procedure is applicable.

The above representation (17) suggests, however, that the no-tension algorithm is a special version of the modified Newton-Raphson method. The Newton-Raphson method and the no-tension algorithm are the two opposite extreme forms of the modified Newton-Raphson method ; where to redefine the stiffness matrix is the only difference among these methods. The most efficient of them is therefore available if we construct a program based upon the modified Newton-Raphson method and control the pace of updating the stiffness matrix appropriately. The computational procedure of the present method is summarized in Appendix Ⅲ.

## 4. NUMERICAL EXAMINATIONS

If a hub attached to a circular and flat elastic membrane at the center is rotated by a torque M, a circular wrinkled region arises around the hub. By virtue of symmetry this problem is solved analytically[2]. A result is shown in Fig. 2 (1) and Fig. 3.

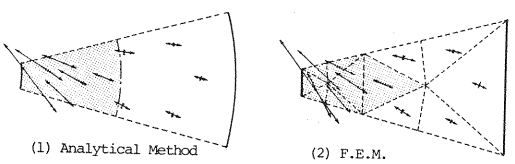


Fig. 2 Stress Field.

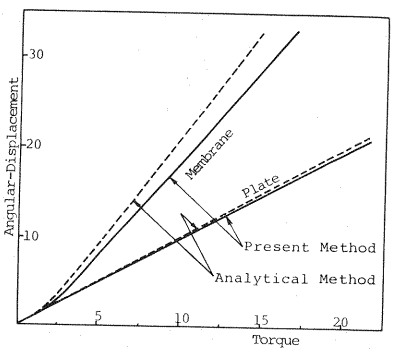


Fig. 3 Load-Displacement Relation.

Relatively coarse finite elements are applied as shown in Fig. 2 (2). If one takes the symmetry of the problem into consideration, one can introduce more elegant elements. Awkward meshes are employed, however, in order to examine the applicability of the present method strictly. As a matter of fact, when it is applied later to the total system, the polyhedral dome, it is practically difficult to define an optimal network to each membrane panel ; rubber-stamp elements are inevitable.

Discrepancy of the description of the tension field area, shadowed in the figure, between the both methods is apparent. The finite elements partition employed here is nearly most improper, because the transversal dividing lines of the elements considerably miss the border line of the tension field, and yet the results of the distribution of principal stress show a good agreement.

Fig. 3 shows the planar angular-displacement of the membrane against the applied torque. The membrane is fixed at the circumference. The value of the torque is normalized with $2\pi R^2 tT$ where $R$ and $t$ are the radius of the hub and the thickness of the membrane. T is the pre-tension of the membrane. The angular-displacement of the hub is normalized, too, so that wrinkling occurs when it is unity. Solid lines indicate the result of the present method and dashed lines are that of the analytical method. For comparison, the result of a corresponding elastic plate, which suffers no wrinkling, is added.

Another example is a shearing problem of a rectangular membrane shown in Fig. 4. The sample is 1.0 m high, 0.8 m wide and 0.001 m thick. Young's modulus is $10^4$t/cm$^2$ ($9.8\times10^8$ kN/m$^2$). Shearing forces are applied to the upper

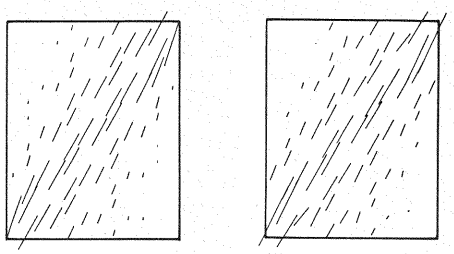


Fig. 4 Stress Field.

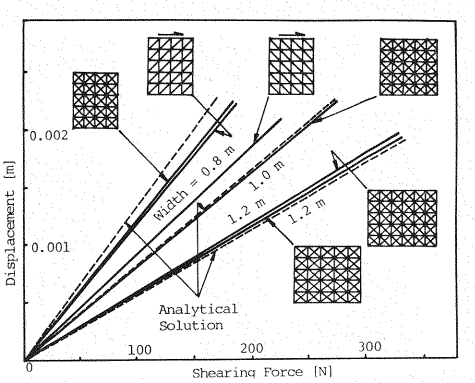


Fig. 5 Load-Displacement Relation.

and lower sides which are restricted to horizontal movements. In this case the principal stress forms straight lines. Fig. 4 (1) is given by an analytical method[3], and Fig. 4 (2) is the result of the present method in which the membrane is divided into 80 triangular elements. The former is solved only numerically ; some error is inevitable.

Fig. 5 shows the relation between the applied force and the relative translation of the upper and lower sides. The width of the rectangle is changed parametrically from 0.8 m to 1.2 m. Applicability of the finite element method significantly depends not only on the finite element partition but also on its fitness to the geometry of wrinkling which is not known beforehand.

## 5. ANALYSIS OF A HEXAGONAL PANEL

As was stated in Chapter 2, our structure is composed of pentagonal or hexagonal panels. In this chapter, a regular hexagonal panel shown in Fig. 6 is investigated. The length of the sides is 1.0 m and the membrane is 0.0012 m thick. Young's modulus and Poisson's ratio are 69 t/cm$^2$ ($6.8\times10^6$ kN/m$^2$) and 0.3, respectively. The model has 54 elements and 37 nodes.

Two adjacent vertices of the panel are fixed. Remaining four vertices move in the plane of the paper. When a normal pressure is applied, the internal nodes move in the normal direction. Six flanges are assumed rigid. All vertices are hinges ; the flanges rotate freely in the plane. Total degree-of-freedom is 60.

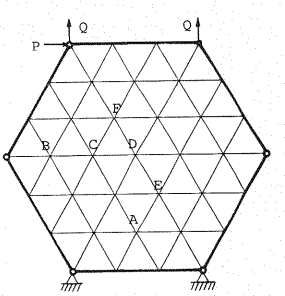


Fig. 6 Model of Panel.

Two types of loads are investigated : symmetrical vertical load $Q$and horizontal load $P$. They apply in the plane of the paper.

(1) Vertical Load

The stiffness of the panel is evaluated with the load-displacement relation. Some examples are given in Fig. 7. It shows the process of incremental loading under the action of a constant normal pressure designated with $p$. The ordinate is the vertical displacement of the upper lateral member. The dashed line indicates the response of an imaginary perfectly elastic membrane which can carry the compressional stress as well as the tensile one. The critical points where the wrinkling occurs are indicated with white circles. If the pressure is zero, any load except zero immediately causes wrinkling. The load-displacement relation is in this case linear. As the load increases, the curves of non-zero pressures gradually approach this line ; the overall stiffness of the panel drops gradually. Fig. 8 illustrates an example of the distribution of the principal stress where the internal pressure is 6 kN/m$^2$.

Normal displacement of the membrane drops from the initial inflated state gradually as the load increases. The example corresponding to Fig. 8 is shown in Fig. 9. The initial configurations of the inflated membrane surface were determined by solving numerically the nonlinear equation of equilibrium of the membrane. The points of reference are shown in Fig. 6. At the first stage it decreases slowly. Then it begins to drop quickly while a large planar displacement occurs simultaneously as is seen in Fig. 7.

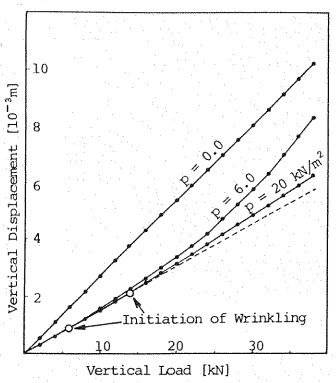


Fig. 7 Load-Displacement Relation.

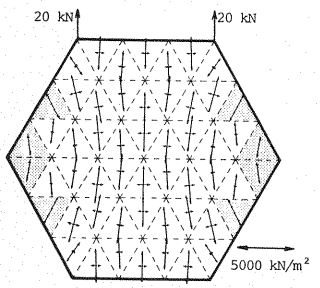


Fig. 8 Stress Field under a Vertical Load.

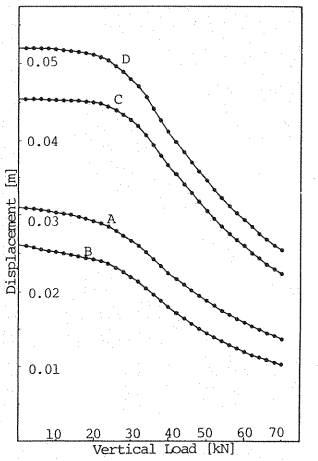


Fig. 9 Normal Displacement.

## ( 2 ) Horizontal Load

Fig. 10 shows the load-displacement relation. The dashed line indicates the response of the imaginary perfect membrane which suffers no wrinkling. The relation is no more linear even if the pressure is zero ; nonlinearity of the finite rotation of the flanges becomes nonnegligible. The relation itself is similar to that of the vertical load. The horizontal load, however, produces far larger displacement. The difference is to be attributed to the geometry of the stress field. In fact, the magnitude as well as the direction of the principal stress are scattered in the panel and relatively small area contributes to the overall stiffness (Fig. 11). Internal pressure of Fig. 11 and Fig. 12 is 5 kN/m$^2$. Normal movement of the internal points is shown in Fig. 12. A similar shape of the curves to the case of the vertical load is seen here, too. They begin to fall when the load a little exceeds 1 ton (9.8 kN).

In order to evaluate the efficiency of the applied iteration procedure, the number of iterations required to get a converged solution to each loading step is counted. An example to the horizontal loading is given in Fig. 13. Some steps require noticeably many iterations ; e. g., the three steps corresponding to the load from 10 to 20 kN. This is briefly explained as follows : at this interval the normal displacement of the membrane begins to drop abruptly as is seen in Fig. 12. The decrement of the displacement to be adjusted by the iteration increases almost suddenly. On the other hand, the tangential stiffness matrix which conducts the adjustment process remains as before ; it modifies the objective values only little by little. The influence of the distribution of the wrinkled area on the required number of iterations is complicated and remains open to further considerations.

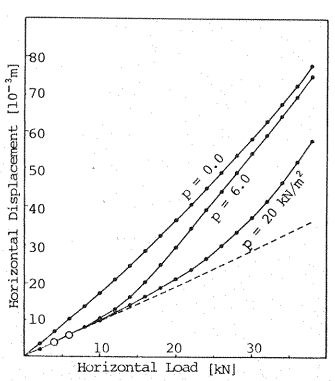


Fig. 10 Load-Displacement Relation.

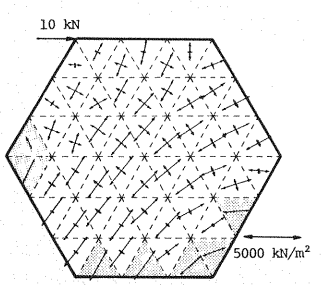


Fig. 11 Stress Field under a Horizontal Load.

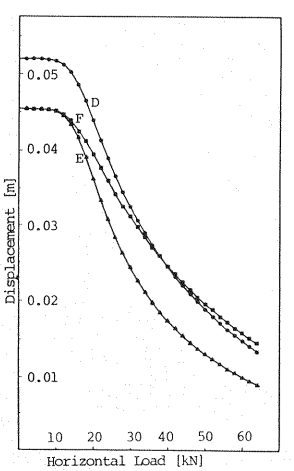


Fig. 12 Normal Displacement.

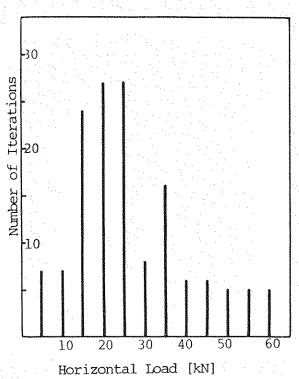


Fig. 13 Number of Iterations.

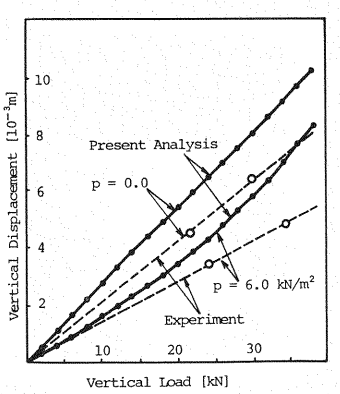


Fig. 14 Comparison with Experimental Data.

Few experimental data have been so far reported. Kato and others investigated the vertical displacement of a regular hexagonal membrane under vertical loads[9]. Although their sample is a little larger than the panel examined above, the results are readily convertible into those under the computational conditions, because the flanges of the panel are approximately rigid. Fig. 14 shows the result of the numerical analysis and the converted result of the experimental work. The former, which is shown with solid lines, is identical to Fig. 7 except for the symbols used. Here the white circles and the dashed lines indicate the experimental results.

It is obvious that the experimental model has significantly larger stiffness than the numerical model. These discrepancies can be attributed to two causes.

(1) Since the flanges of the experimental panel was fabricated as one body with the web membrane, the vertices have some nonnegligible stiffness against the planar relative rotation of two adjacent flanges.

(2) The membrane material of the experimental model is to some extent resistible to wrinkling.

Whether these secondary stiffness must be introduced explicitly into the numerical model or not still remains to further studies, because too much complicated computation must be avoided in design practice.

Influence of the other material properties mentioned in Chapter 3 cannot be evaluated by the present method : plasticity, anisotropy and viscoelasticity.

## 6. APPLICATION TO A MODEL DOME

The method developed hitherto is now applied to a dodecahedral dome shown in Fig. 15. One bottom face is attached to the base. Remaining eleven faces are regular pentagons made of the same material as is discussed in Chapter 5. The same postulates are also employed. If the vertices are perfect hinges, the dome is as itself kinematically unstable ; indtroduction of stiffness by the internal pressure is essential.

Six internal nodes are assigned to each panel : one at the center and the others so as to form a concentric regular pentagon around the center (cf. Fig. 17). This degree-of-freedom appears to be necessary to detect the influence of wrinkling. Total degree-of-freedom amounts to 348.

Two types of nodal forces are applied : vertical and horizontal. The former is applied to the five nodes of the top panel. Since the load is axisymmetry-like, the top panel never deforms. Fig. 16 shows the vertical displacement of the vertices of the top panel. So long as the applied force remains less than about 20 kN, effect of the pressure can be evaluated as linear. All the inclined panels suffer an identical deformation. There is

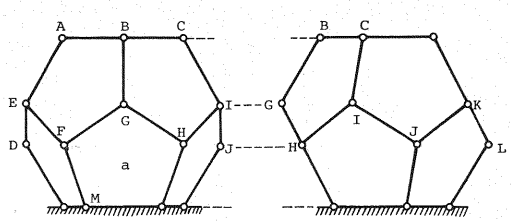


Fig. 15 Model Polyhedral Dome.

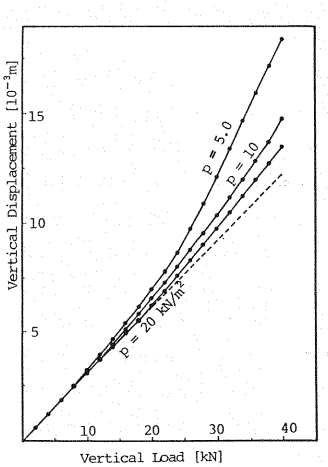


Fig. 16 Load-Displacement Relation.

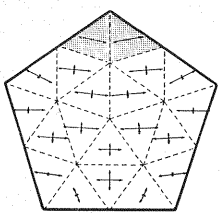

Fig. 17 Stress Field of a Panel.

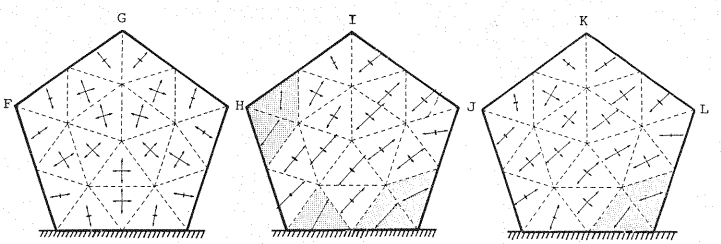


Fig. 18 Stress Field of Lower Panels.

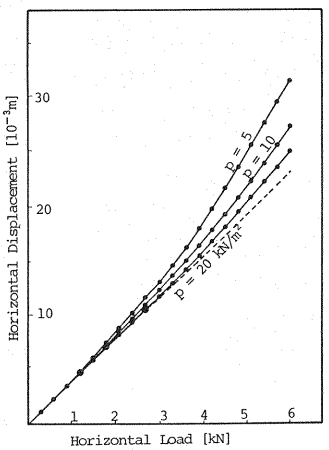


Fig. 19 Load-Displacement Relation.

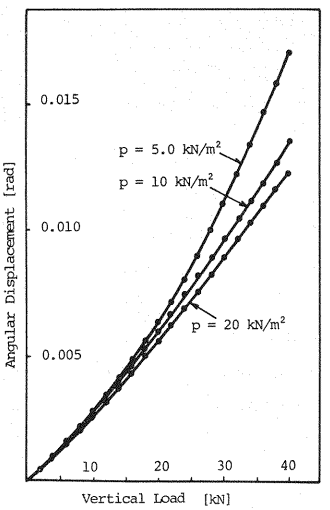


Fig. 20 Angular Displacement of Bending Type.

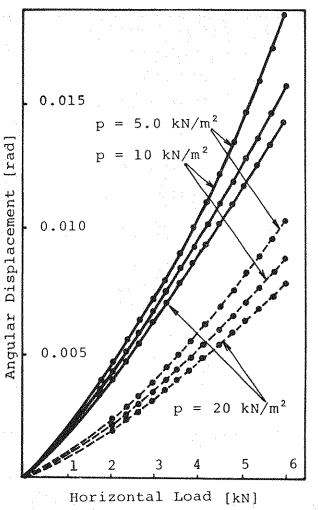


Fig. 21 Angular Displacement of Torsion Type.

vertical contraction accompanied by the swelling of the intermediate nodes ; accordingly, the primary principal stress is nearly horizontal as is shown in Fig. 17. Wrinkling occurs only in the neighborhood of the intermediate vertices.

Next, same horizontal forces are applied to the nodes A～J of Fig. 15. The deformation has therefore plane symmetry. The dome deforms primarily like a cantilever ; a composite of bending and shearing type. Since it has a sphere-like, short and thick configuration, the latter type is expected to be prevailing. The overall stiffness against the shearing force is well indicated with the horizontal displacement of the upper nodes (Fig. 19) . The figure suggests considerably small stiffness against the shearing forces. These forces impose a large deformation upon the lower panels except the front face designated as "a" in Fig. 15. As is shown in Fig. 18, these panels really experience a large shearing deformation. The upper panels as well as the front panel carry no large stress. In practice, the horizontal force representing the wind load is far larger than the vertical ones representing the dead load and the snow load. Strength of the lower panel is therefore of highest importance. Since the model employed is very small, the wind load is absolutely small. More realistic models with much more vertices are desirable for wind-resistant design.

In practice, design of the nodal points is most important. Angular displacement of the neighboring flanges is therefore most informative. They can be reduced to two components : bending and torsion. In the panel "a" of the model shown in Fig. 15, for example, the former is the change of the angle $\angle FGH$ and the latter is the angle of rotation of the flange $\overline{GH}$ around the axis $\overline{FG}$. This angle of rotation is not identical to that which is measured in the absolute coordinate system, because the flange $\overline{FG}$ rotates around itself. The angle between the projections of $\overline{GH}$ and $\overline{FM}$ on the plane perpendicular to $\overline{FG}$ is therefore employed as an indicator of the torsional displacement. Fig. 20 and Fig. 21 show the cases of the vertical load and the horizontal load, respectively. In Fig. 21, dashed lines indicate the torsional displacement. In case of the vertical load, the torsional displacement is negligibly small ;

accordingly, the panel which is initially a flat plane remains nearly flat and suffers little warping. The solid lines show the increment of the angle $\angle FGH$. These angular displacements are the maxima ; i. e., those of the remaining nodal points are less than or at most equal to them. These results give suggestions on the required durability or stiffness of the nodal points of the flanges.

## 7. CONCLUSIONS

Finite element method has been applied to the wrinkling problems of flat or curved elastic membranes. Ordinary iteration procedures have been proved to yield satisfactory results without special computational difficulties. It was shown that the conventional no-tension algorithm was an incremental form of a fixed-point type equation ; it is representable as a particular version of the modified Newton-Raphson method.

In case of the simple problems which have been solved analytically, the solutions of the present method agree well with the analytical solutions.

The proposed program was applied to a polygonal membrane element and then to the dome itself. The numerical solutions were compared with experimental data given by other investigators. The discrepancy is practically permissible and the numerical solutions give conservative estimations of the structure. These errors are attributable to the bending stiffness of the frames of the membrane panel at the vertices which has been neglected in the analysis and to the stiffness of the membrane material against the compressional forces.

Since the program based upon the theory presented here is not yet well developed toward the analysis of the total system, only a dodecahedral dome was investigated. Overall stiffness of the structure and deformation of the nodal points which are the basic data for the design practice were discussed. The analysis of the miniature model presented here cannot give full informations of the actual structures which are supposed to have hundreds of vertices. More realistic and practically sufficient model study will be available, however, only if the capacity of the program developed here is extended.

## Appendix I. Notations

$x, y$ : rectangular coordinates on the panel plane
$\{u\}=(u_1, u_2)$ : planar displacement of the membrane surface
$\{u\}_e$ : planar displacement in the finite element e
$w$ : normal displacement
$\{\varepsilon_0\}$ : planar strain
$\varepsilon_1, \varepsilon_2$ : principal strains
$\{\varepsilon_*\}$ : nonlinear component of the strain
$\{f\}=(f_1, f_2)$ : external force
$\{\sigma_0\}$ : planar component of the stress
$\sigma_1$ : maximum principal stress
$\theta$ : angle between the direction of the maximum principal stress and the $x$-axis
$\{\Theta\}=(\cos^2\theta,\ \sin^2\theta,\ \sin\theta\cos\theta)^T$
$\nu$ : Poisson's ratio
$E$ : Young's Modulus
$[B]$ : matrix of the strain-displacement relation
$[D]$ : matrix of the constitutive relation
$[A], [G]$ : transformation matrices defined in Eq. (10)
$[K]$ : stiffness matrix of a perfectly elastic body
$[K]_0$ : Jacobian matrix
$[K]_*$ : tangent stiffness matrix
$\{k\}$ : vector-valued nonlinear algebraic operator

## Appendix II. Tangent Stiffness Matrix

The contribution of an element e to the tangent stiffness matrix is represented as an integral of a density matrix $[k]$ over $e$ ; i. e.

$$[K]_e=\int\int_e t\,[k]\,dS_e \quad \cdots\cdots (19)$$

where t is the thickness of the membrane.

If there is no wrinkling in e,

$$[k]=[G]^T\begin{bmatrix}\sigma_x & \tau_{xy}\\ \tau_{xy} & \sigma_y\end{bmatrix}[G]+([B]+[A][G])^T[D]([B]+[A][G]). \quad \cdots\cdots (20)$$

If wrinkling occurs in e,

$$[k]=[G]^T\begin{bmatrix}\sigma_x & \tau_{xy}\\ \tau_{xy} & \sigma_y\end{bmatrix}[G]+([B]+[A][G])^TE([H]+\{\theta\}\{\theta\}^T)([B]+[A][G]). \quad \cdots\cdots (21)$$

In this case, $\{\sigma\}=\sigma_1\{\theta\}$ $\cdots\cdots (22)$

and $$[H]=\frac{1}{2\{(\varepsilon_x-\varepsilon_y)^2+\gamma_{xy}^2\}^{1.5}}\begin{bmatrix}\gamma_{xy}^2 & -\gamma_{xy}^2 & -(\varepsilon_x-\varepsilon_y)\gamma_{xy}\\ -\gamma_{xy}^2 & \gamma_{xy}^2 & (\varepsilon_x-\varepsilon_y)\gamma_{xy}\\ -(\varepsilon_x-\varepsilon_y)\gamma_{xy} & (\varepsilon_x-\varepsilon_y)\gamma_{xy} & (\varepsilon_x-\varepsilon_y)^2\end{bmatrix} \quad \cdots\cdots (23)$$

$(\sigma_x, \sigma_y, \tau_{xy})$ and $(\varepsilon_x, \varepsilon_y, \gamma_{xy})$ are the stress and the strain of the membrane, respectively.

## Appendix III. Computational Procedures

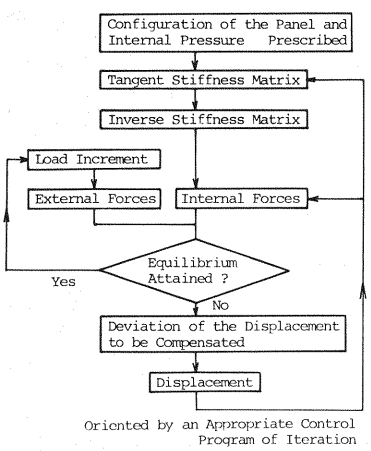


## REFERENCES


1) Otto, F. : Tensile Structures, The M. I. T. Press, 1967.
2) Stein, M. and Hedgepeth, J. M. : Analysis of partly wrinkled membranes, NASA, T. N. D-813, 1961.
3) Mansfield, E. H. : Tension field theory, Proc. 12th Int. Cong. of Applied Mechanics, pp. 305~320, 1968.
4) Mansfield, E. H. : Load transfer via a wrinkled membrane, Proc. Roy. Soc London, A-316, pp. 269~289, 1970
5) Moriya, K. and Umemura, M. : An analysis of the tension field after wrinkling in flat membrane structure, Proc. IASS Sympo., pp. 189~198, 1971.
6) Wu, C. H. and Canfield, T. R. : Wrinkling in finite plane-stress theory, Quart. of Applied Mathematics, pp. 179~199, 1981.
7) Wagner, H. : Ebene Blechwandträger mit sehr dünnem Stegblech, Zeits. für Flugtechnik und Motorluftschiffahrt, 20~8 12, pp. 200~314, 1929.
8) Reissner, E. : On tension field theory, Proc. 5th Int. Cong. of Applied Mechanics, pp. 88~92, 1938.
9) Kato, Y., Amano, K. and Watanabe, I. : Polyhedral Radome of 17 m Diameter, Kyoka Plastics (Reinforced Plastics) vol. 27, No. 6, pp. 223~229, 1980 (in Japanese).
10) Higashihara, H. and Shimizu, T. : A study on a flat membrane-frame structure, Proc. Ann. Meeting, ASCE, 35- I -23, pp. 45~46, 1980 (in Japanese).
11) Honma, T. and Tosaka, N. : Analysis of the tension field by the finite element method, Proc. 15th Sympo. of Matrix Method, pp. 287~292, 1981 (in Japanese).
12) Zienkiewicz, O. C., Valliappan, S. and King, I. P. : Stress analysis of rock as a no-tension material, Geotechnique, 18, pp. 56~66, 1968.


(Recieved September 21, 1983)